Acta Crystallographica Section B
Structural Science
ISSN 0108-7681

Variable-temperature studies of the 4-isopropylphenol crystal structure from X-ray diffraction. Comparison of thermal expansion and molecular dynamics with spectroscopic results

Grażyna Wójcik* and Jolanta Holband

Institute of Physical and Theoretical Chemistry, Wrocław University of Technology, Wyb. Wyspiańskiego 27, 50-370 Wrocław, Poland

Correspondence e-mail: wojcik@kchf.ch.pwr.wroc.pl

Received 10 October 2001
Accepted 11 March 2002

Crystalline 4-isopropylphenol, $C_9H_{12}O$, an optically non-linear material, was studied by X-ray diffraction in order to determine its structure at several temperatures in the 95–300 K range. The thermal expansion coefficients have been calculated from the lattice parameters' dependence on temperature. The rigid-body analysis of the anisotropic displacement parameters including the correlation with the internal motion of large amplitude provided the values of the molecular translation and libration tensors at the temperatures studied and was used to characterize the torsional motion of the isopropyl group. The calculated normal modes and internal torsion frequency were compared with the wave numbers at the maximum of bands in the low-frequency Raman scattering, FTIR and inelastic neutron scattering spectra.

1. Introduction

Crystalline 4-isopropylphenol (IP) was studied in the 1970s and 1980s, when its crystal structure (Perrin *et al.*, 1977) and second-harmonic generation with an efficiency 50 times greater than in quartz (Perrin *et al.*, 1983) were reported. Recently, this material drew attention as an interesting example for structure *versus* non-linear optical properties relationship studies. The experimental and theoretical investigations of vibrational and electronic spectra of solid IP measured in different environments made a proposal for the assignments of the observed bands possible and revealed the existence of intermolecular charge transfer along the direction of the hydrogen bond which links the molecules into a helix. This charge transfer seems to couple with some molecular vibrations (Szostak *et al.*, 1995). Our recent publication dealt with thermally activated molecular reorientations in solid IP studied by dielectric relaxation and other methods. These multi-method investigations indicated the dramatic increase of molecular dynamics from above room temperature coupled with growing electric conductivity. Also the occurrence of a high-temperature, probably disordered, phase was observed. The intermolecular hydrogen bonds of medium strength turned out to be preserved until the melting and, even stronger, they occurred in the high-temperature phase (Wójcik *et al.*, 1999).

The objective of this work was to determine the IP crystal structure at several temperatures over a wide temperature range in order to explore possible structure changes as well as molecular interactions and dynamics through thermal expansion and rigid-body analysis of anisotropic displacement parameters (Cruickshank, 1956; Schomaker & Trueblood, 1968). The rigid-body analysis including the correlation of internal vibration of large amplitude (*e.g.* Dunitz & White, 1973; Dunitz *et al.*, 1988; Schomaker & Trueblood, 1998) was

© 2002 International Union of Crystallography
Printed in Great Britain – all rights reserved

used with the aim of characterizing the torsional vibration of the isopropyl moiety of the IP molecule, namely, to obtain the amplitudes, frequencies and potential barriers to the motion at the temperatures studied. The normal modes of molecular translations and librations from the rigid-body analysis as well as the internal torsion frequency (calculated within harmonic approximation) have been compared with the results from other methods, namely, the low-frequency Raman scattering and FTIR spectra (Misiaszek *et al.*, 1995), the inelastic incoherent neutron scattering spectra and the MNDO calculations for the hydrogen-bonded dimer (Hołderna-Natkaniec *et al.*, 1996).

2. Experimental

Commercial (Aldrich) pure IP was further purified by sublimation under vacuum and multiple-zone refinement. The final product melted at 333 K. Single-crystal specimens, suitable for X-ray diffraction, were grown from a hexane solution. Depending on the crystallization conditions we also obtained the crystals in the form of long needles, which apparently represented the high-temperature disordered phase of IP (Wójcik *et al.*, 1999). Owing to the enormous amount of sublimation taking place, the single-crystal samples had to be put into glass capillaries. The X-ray diffraction measurements were performed on a KUMA Diffraction four-circle automatic diffractometer equipped with an area detector and an Oxford Cryosystems cooling unit. Mo $K\alpha$ radiation (λ = 0.71073 Å) was used. The measurements were performed for two crystal specimens measured at temperatures 95, 110, 140, 250 K and 163, 173, 180, 193, 198, 200, 300 K, respectively. The precision of the temperature stability was 0.1 K. During the data collection ω scans were performed. No absorption corrections were used. Data reductions were performed with *KM4CCD* software (Kuma Diffraction, 1999). The structures were solved by direct methods (Sheldrick, 1990) and refined by least-squares methods with the programs from the *SHELXL97* package (Sheldrick, 1997). Atomic scattering factors were taken from *International Tables for Crystallography* (1992, Vol. C, Tables 4.2.6.8 and 6.1.1.4). The H atoms were found using a riding model and were refined isotropically. Other details of the data collection and the refinement for the three temperatures chosen are shown in Table 1.[1] The rigid-body analysis (Cruickshank, 1956; Schomaker & Trueblood, 1968; Dunitz & White, 1973), including the correlation of the internal motion of the non-rigidly attached rigid group (Dunitz *et al.*, 1988; Schomaker & Trueblood, 1998), was performed with *THMA11* (Farrugia, 1998).

3. Results and discussion

3.1. Crystal structures at different temperatures

The IP crystal belongs to the $P4_1$ (or $P4_3$) space group as was first established by Perrin and co-workers (Perrin *et al.*, 1977). The structure does not reveal any spectacular changes between 95 and 300 K. The hydrogen-bonded molecules are packed in the form of helices about the fourfold screw axes as shown in Fig. 1. The intermolecular O···O distance varies from 2.750 Å at 95 K to 2.818 Å at 300 K and the respective values for the H···O distance are 1.914 Å and 2.004 Å. The molecule is planar except for two methyl groups which are twisted from the molecular plane. The two C atoms from the methyl groups lie at angles of about 80° to the plane through the phenyl ring. The molecular conformation shows no significant changes with variation of temperature. The C3—C4—C7—C9 torsional angle varies from 51.7° to 53.6° over the temperature range studied. There are no signs of quinoid structure contribution in the IP molecule. This result is consistent with the spectroscopic observations and quantum-chemical calculations of the molecular dipole moments (Szostak *et al.*, 1995).

The thermal evolution of the unit-cell parameters is shown in Fig. 2. The *c* dependence is not smooth. On the other hand, the *a* curve forms a wide shallow minimum between 100 and 200 K. At the moment we are not able to decide whether these features of the dependence are relevant. Nevertheless, a small anomaly looking like a 'lambda'-type transition had been previously observed at around 180 K on the differential scanning calorimetry cooling and heating curves (Wójcik *et al.*, 1995). What is more, at a temperature of around 180 K a highly anharmonic increase in libration about the long molecular axis has been revealed by the rigid-body analysis as is shown in Fig. 5. The principal thermal expansion coefficients, calculated from the temperature dependence of the unit-cell parameters, are reported in Table 2. Their values can be compared with the thermal expansion coefficients of other

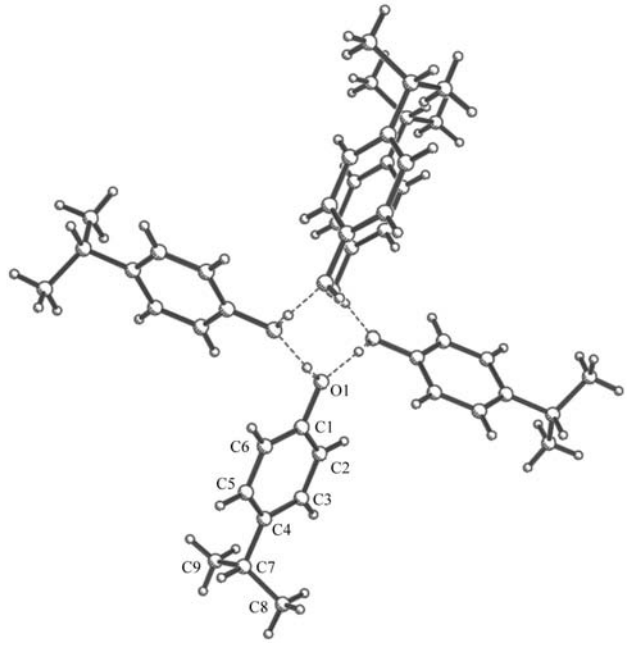

Figure 1
ORTEP3 (Farrugia, 1997) view of molecular packing in the IP crystal along the fourfold screw axis with atom numbering.

[1] Supplementary data for this paper are available from the IUCr electronic archives (Reference: NS0008). Services for accessing these data are described at the back of the journal.

Table 1
Experimental details.

	95 K	180 K	300 K
Crystal data			
Chemical formula	$C_9H_{12}O$	$C_9H_{12}O$	$C_9H_{12}O$
Chemical formula weight	136.19	136.19	136.19
Cell setting, space group	Tetragonal, $P4_1$	Tetragonal, $P4_1$	Tetragonal, $P4_1$
a, b, c (Å)	9.848 (3), 9.864 (3), 8.166 (2)	9.859 (2), 9.865 (2), 8.221 (1)	9.928 (1), 9.934 (1), 8.316 (1)
V (Å^3)	793.3 (4)	799.6 (2)	820.16 (15)
Z	4	4	4
D_x (Mg m^{-3})	1.140	1.131	1.103
Radiation type	Mo $K\alpha$	Mo $K\alpha$	Mo $K\alpha$
No. of reflections for cell parameters	887	1091	1535
μ (mm^{-1})	0.072	0.072	0.070
Temperature (K)	95 (2)	180 (2)	293 (2)
Crystal form, colour	Prism, colourless	Prism, colourless	Prism, colourless
Crystal size (mm)	0.72 × 0.44 × 0.29	1.02 × 0.51 × 0.36	1.02 × 0.51 × 0.36
Data collection			
Diffractometer	Kuma Diffraction KM4CCD diffractometer	Kuma Diffraction KM4CCD diffractometer	Kuma Diffraction KM4CCD diffractometer
Data collection method	ω scans	ω scans	ω scans
No. of measured, independent and observed parameters	5936, 2162, 2018	4181, 1453, 1281	4448, 1519, 1049
Criterion for observed reflections	$I > 2\sigma(I)$	$I > 2\sigma(I)$	$I > 2\sigma(I)$
R_{int}	0.0636	0.0424	0.0447
θ_{max} (°)	31.15	31.33	31.29
Range of h, k, l	$-13 \rightarrow h \rightarrow 11$ $-14 \rightarrow k \rightarrow 14$ $-11 \rightarrow l \rightarrow 10$	$-14 \rightarrow h \rightarrow 14$ $-13 \rightarrow k \rightarrow 14$ $-12 \rightarrow l \rightarrow 7$	$-14 \rightarrow h \rightarrow 14$ $-14 \rightarrow k \rightarrow 14$ $-12 \rightarrow l \rightarrow 8$
Refinement			
Refinement on	F^2	F^2	F^2
$R[F^2>2\sigma(F^2)]$, $wR(F^2)$, S	0.0598, 0.1495, 1.095	0.0593, 0.1684, 1.199	0.0603, 0.1844, 1.104
No. of reflections and parameters used in refinement	2162, 92	1453, 93	1519, 90
H-atom treatment	Mixed	Mixed	Mixed
Weighting scheme	$w = 1/[\sigma^2(F_o^2) + (0.0684P)^2 + 0.4970P]$ where $P = (F_o^2 + 2F_c^2)/3$	$w = 1/[\sigma^2(F_o^2) + (0.0956P)^2 + 0.1106P]$ where $P = (F_o^2 + 2F_c^2)/3$	$w = 1/[\sigma^2(F_o^2) + (0.1050P)^2 + 0.0244P]$ where $P = (F_o^2 + 2F_c^2)/3$
$(\Delta/\sigma)_{max}$	0.002	0.000	0.001
$\Delta\rho_{max}$, $\Delta\rho_{min}$ (e Å^{-3})	0.286, −0.395	0.337, −0.397	0.218, −0.193
Extinction method	None	*SHELXL*	*SHELXL*
Extinction coefficient	0	0.32 (5)	0.34 (5)

Computer programs used: *SHELXS*97 (Sheldrick, 1990), *SHELXL*97 (Sheldrick, 1997), *KM4CCD* (Kuma Diffraction, 1999).

Table 2
Principal thermal expansion coefficients (deg^{-1}).

	110 K	300 K
$\alpha_1 = \alpha_2$ ($\perp$ **c**)	-2.43×10^{-5}	8.88×10^{-5}
α_3 ($\parallel$ **c**)	8.05×10^{-5}	8.05×10^{-5}

molecular crystals with intermolecular hydrogen bonds, *e.g. m*-nitroaniline (Wójcik & Holband, 2001), DCNP (Cole *et al.*, 2000), *m*-nitrophenol (Wójcik *et al.*, 1992), thiourea (Jakubowski & Ecolivet, 1980) and *p*-nitroaniline (Rohleder *et al.*, 1971). The α_{33}, *i.e.* the principal thermal expansion coefficient along the *c* axis, has to be correlated with the hydrogen bond which links molecules into helices along the *c* axes. It seems that, preserving the H bonds, the molecules exhibit thermal motions of large amplitudes along the *c* direction. These motions could be molecular translations and librations as well as torsional vibrations of the isopropyl moieties. Fig. 3 shows the IP molecule with atomic displacement ellipsoids drawn at the 50% probability level at three temperatures: 95, 180 and 300 K.

3.2. Rigid-body analysis of anisotropic displacement parameters with correlation of internal motion

The elements of the rigid-body **T** (translation), **L** (libration) and **S** (correlation between molecular translations and librations in the case of a non-centrosymmetric molecule) tensors in the inertial axes frame are presented in Table 3. The estimated standard deviations of the calculated values of the **T**, **L** and **S** tensors are in the range from 10 to 20%. The quality of the calculated values is estimated by the reliability index, the *wR* factor, which is calculated as in the crystal structure refinement. The *wR* factor (given in Table 3) shows the discrepancy between the values of the anisotropic displacement parameters used in the rigid-body analysis and the

values recalculated from the previously calculated **T**, **L** and **S** tensors (Trueblood, 1978). In Fig. 4 the inertial axes system related to the IP molecule together with the crystallographic axes system are shown. The I_1 inertial axis lies along the long molecular axis, the I_2 axis is perpendicular to I_1 and lies in the phenyl ring plane, and the I_3 axis is perpendicular to both I_1 and I_2 in the right-hand system of axes. Fig. 5 shows the variation of the principal values of the **T** and **L** tensors with temperature. The principal values of the libration tensor, $\mathbf{L}_1$, $\mathbf{L}_2$, $\mathbf{L}_3$, correspond to librations about axes which lie near to the inertial axes I_1, I_2 and I_3. The libration about the long molecular axis is the most pronounced molecular motion. The

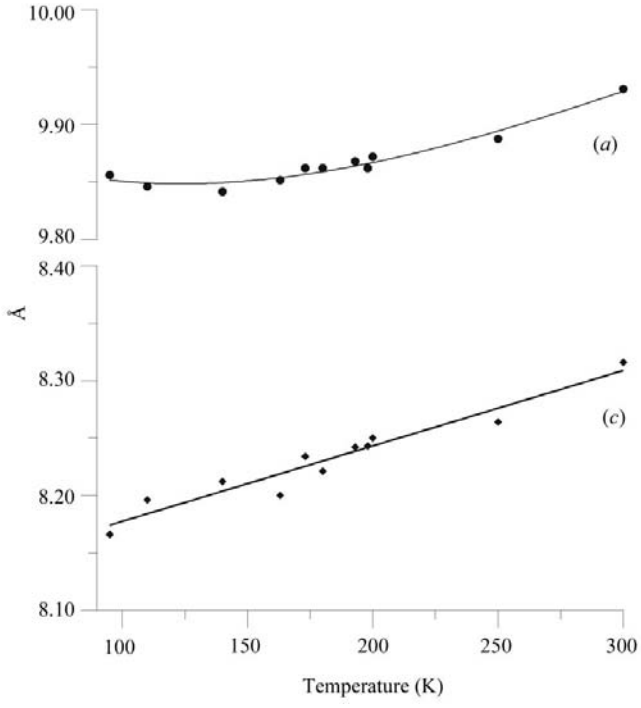

Figure 2
The variation of the IP lattice parameters with temperature. The estimated standard deviations of the lattice parameters are in the range from 0.001 to 0.003 Å. Solid lines serve as guides to the eye.

Table 3
The values of the rigid-body **T** (Å^2), **L** (deg^2) and **S** (rad Å) at temperatures 95 K, 180 K and 300 K in the inertial coordinate system.

Further information is given in the text.

		95 K	180 K	300 K
T (Å^2)	T^{11}	0.01515	0.02800	0.05215
	T^{12}	−0.00029	0.00103	−0.00119
	T^{13}	−0.00142	−0.00138	−0.00068
	T^{22}	0.01320	0.02226	0.04290
	T^{23}	−0.00043	−0.00140	0.00255
	T^{33}	0.01338	0.02550	0.04804
L (deg^2)	L^{11}	19.351	27.667	49.825
	L^{12}	−1.764	2.492	−3.514
	L^{13}	−0.434	−0.634	4.535
	L^{22}	6.502	9.702	16.675
	L^{23}	−1.101	1.665	−3.022
	L^{33}	1.747	3.669	7.199
S (rad Å)	S^{11}	0.00017	−0.00001	−0.00019
	S^{12}	−0.00051	−0.00025	−0.00041
	S^{13}	0.00165	−0.00281	−0.00425
	S^{21}	−0.00004	−0.00003	0.00022
	S^{22}	−0.00064	0.00085	0.00188
	S^{23}	−0.00158	−0.00259	0.00503
	S^{31}	−0.00002	0.00003	−0.00006
	S^{32}	0.00058	0.00109	−0.00229
	S^{33}	0.00047	−0.00084	−0.00169
wR†		0.057	0.059	0.045

† $wR = [\Sigma w(U^{ij}{}_o - U^{ij}{}_c)^2/\Sigma w U^{ij}{}_o{}^2]^{1/2}$; $w = \sigma[\langle U^{ij}{}_o\rangle]^{-2}$.

amplitude is larger than the largest libration amplitude of the *m*-nitroaniline molecule, which also occurs about the long molecular axis. It is relatively high even at 95 K. This behaviour may originate from rather low crystal density. The translation amplitudes along the three perpendicular directions are comparable, the $\mathbf{T}_1$ values being slightly higher. They are also comparable with the translation amplitudes of *m*-nitroaniline (Wójcik & Holband, 2001). The values of the reliability index, *wR*, reported in Table 3 indicate that the contributions of the internal vibrations to the anisotropic displacement parameters determined by X-ray diffraction at 95 and 180 K are similar and this contribution is less at 300 K (Hummel *et al.*, 1990). This contribution may originate from

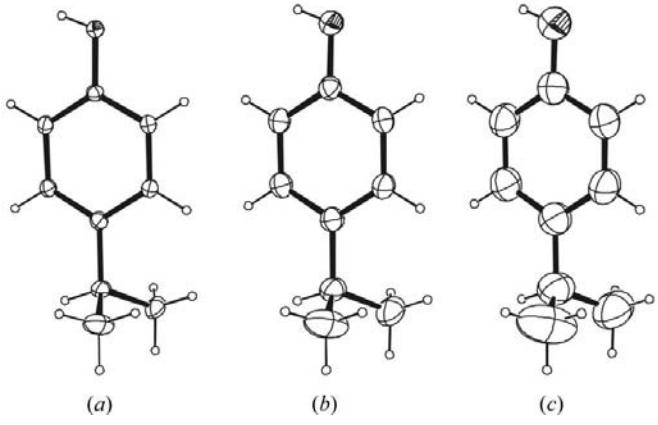

Figure 3
The IP molecule with the displacement ellipsoids drawn at the 50% probability level at 95 K, 180 K and 300 K.

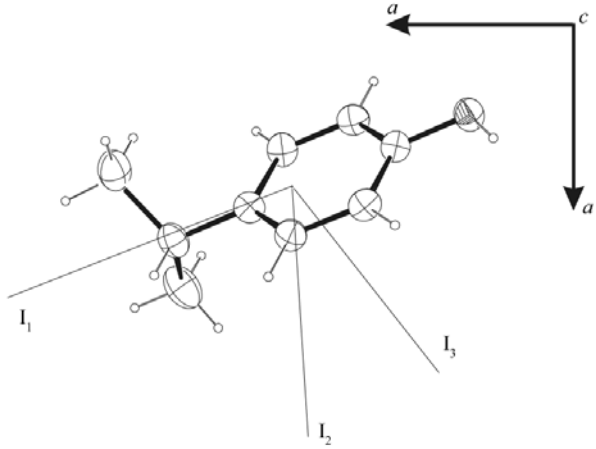

Figure 4
The orientation of the inertial and crystallographic axes with respect to the IP molecule.

the methyl groups' vibrations but, being refined isotropically, the H atoms have not been included in the rigid-body analysis.

The correlation of the internal motion of large amplitude with the rigid-body translations and librations enabled us to examine the torsional vibration of the isopropyl moiety of the IP molecule. The procedure involved in *THMA11* provided the amplitude of the rigid-body libration about the C4—C7 bond which links the isopropyl group to the phenyl ring and the amplitude of the overall (libration plus torsion) motion of the group about the same axis. The two amplitudes are shown in Fig. 6 as a function of temperature. The amplitude of the rigid-body libration about the axis of the torsion and the amplitude of torsion, the two motions about the same axis in which the isopropyl group is involved, are of the same order of magnitude. Hence, their contribution to the thermal expansion of the IP crystal should be similar.

3.3. Rigid-body normal modes and torsion frequency and their comparison with wave numbers from optical spectroscopy and inelastic neutron scattering

Calculated within harmonic approximation the rigid-body normal modes represent average values from the first Brillouin zone (Bürgi, 1995). The three translations and three librations have the following frequency values (average for 11 temperatures measured): 33, 35, 38, 53, 66 and 86 cm^{-1}. The internal torsion frequency of the isopropyl group is 111 cm^{-1} (the average value for ten temperatures in the 110 to 300 K range), while the potential barrier for the torsion ranges from 80 to 140 kJ mol^{-1}. The variation of the normal mode frequencies with temperature is quite smooth. This is not the case for the frequency of the internal torsion whose value shows 10% to 20% deviations from the average at the different temperatures. The frequency values can be significantly different from the values found for the optical spectra which refer to the centre of the Brillouin zone. In the case of a non-centrosymmetrical crystal (such as IP) the translation and libration modes mix according to the group theory (Turrell, 1972). For the IP crystal (C_4 point group and four molecules in the unit cell) we expect 16 optical lattice modes and 19 (16 optical plus three acoustic) modes in the inelastic neutron scattering spectrum. The frequencies found in the inelastic incoherent neutron scattering (IINS) spectra correspond to the entire Brillouin zone. Table 4 contains the frequencies (in cm^{-1}) of normal modes and internal torsion from the rigid-body analysis, the wave numbers of weighted phonon density of states in the IINS spectra (Hołderna-Natkaniec *et al.*, 1996), as well as the wave numbers from the low-frequency Raman scattering and FTIR spectra (Misiaszek *et al.*, 1995). The frequency values calculated by the MNDO method for the hydrogen-bonded molecular dimer (Hołderna-Natkaniec *et al.*, 1996) corresponding to the discussed frequency range are also reported. The agreement of the frequency values obtained by the different methods is quite good and can facilitate the assignments of frequencies observed in the spectra.

4. Conclusions

The variable-temperature rigid-body analysis of anisotropic displacement parameters seems to be a relatively simple method for obtaining insight into thermally activated mole-

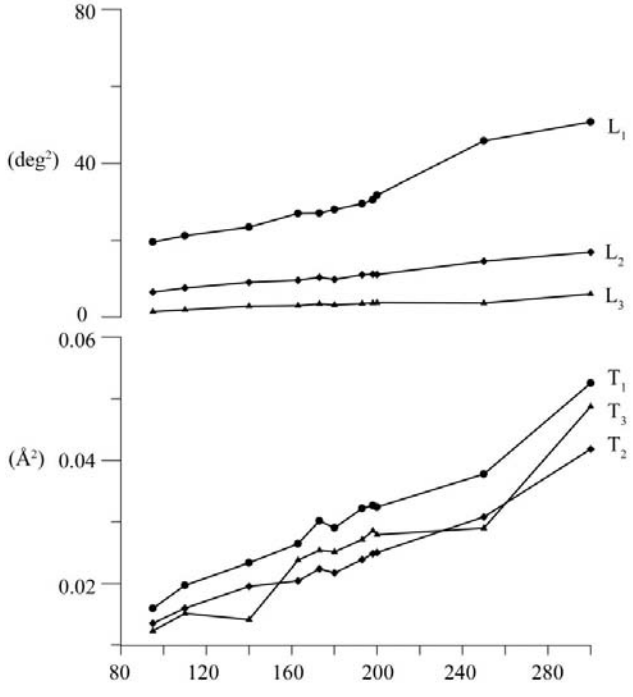

Figure 5
The thermal evolution of the principal values of the translation and libration tensors. For further information see the text. Solid lines serve as guides to the eye.

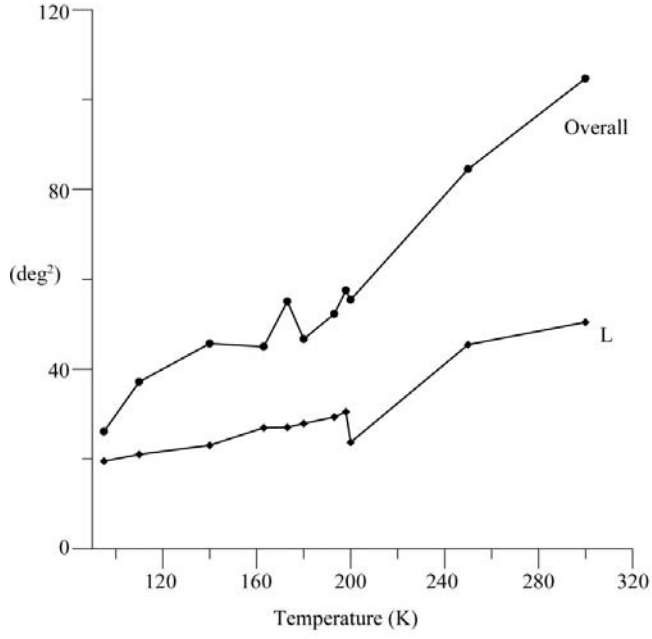

Figure 6
The temperature dependence of the amplitudes of the overall (upper curve) and libration (bottom curve) motions of the isopropyl group about the C_4—C_7 bond. Solid lines serve as guides to the eye.

Table 4
Normal modes and internal torsion frequency from rigid-body analysis (this work), frequencies at the maximum of bands in Raman scattering, FTIR (Misiaszek *et al.*, 1995) and IINS low-frequency spectra and frequencies calculated by the MNDO method for a molecular dimer (Hołderna-Natkaniec *et al.*, 1996).

w – weak; m – medium; s – strong intensity of a band. RT – room temperature.

	Wave numbers (cm^{-1})			
Rigid-body normal modes and internal torsion†	IINS (9 K)	MNDO	Raman‡ (RT)	IR (RT)
33 ($\mathbf{T}_1$)	20	17.49	–	–
35 ($\mathbf{T}_2$)	30	29.91	36.5 (w)	–
38 ($\mathbf{T}_3$)	40	41.50	41.5 (s)	44 (s)
53 ($\mathbf{L}_1$)	43	42.98	52 (s)	53 (m)
66 ($\mathbf{L}_2$)	65	64.66	63 (w)	65 (m)
88 ($\mathbf{L}_3$)	85	84.60	75 (w)	75 (m)
–	90	90.11	90 (w)	86 (m)
–	–	–	97 (w)	96 (m)
111 (τ)	106	–	104 (s)	103 (s)
–	–	–	113 (w)	110 (s)
–	125	124.42	123 (m)	125 (s)

† Average values from the 95–300 K range. ‡ Average for all polarizations.

cular dynamics in the crystalline state, especially in the case of missing lattice dynamics calculations. The most pronounced molecular motion in the crystalline IP turned out to be the libration about the long molecular axis. This motion, coupled with the torsional vibration of the isopropyl moiety, may contribute to the non-linear optical properties of the material. According to the model given by Oudar & Chemla (1975), the non-linear optical properties of benzene derivatives originate from intramolecular charge transfer between electron-donating and electron-accepting substituents to the phenyl ring. IP molecules contain only one heteroatom and the hydroxyl group acts as an electron donor. The role of an electron acceptor towards the hydroxyl group is adopted by the phenyl ring which also acts as an electron donor towards the isopropyl group (Szostak *et al.*, 1995). This polarization mechanism may be coupled with the molecular libration with its amplitude parallel to the polar axis along the hydrogen-bond direction. As was recently discussed in the case of DCNP, another optically non-linear organic material, the phenyl librations may enhance the charge transfer along the hydrogen-bond direction and contribute to the second-harmonic generation effect (Cole *et al.*, 2000). The frequencies of normal modes and internal torsion calculated from the rigid-body amplitudes agree with the frequencies found in the optical and IINS spectra and those calculated for the hydrogen-bonded dimer by the MNDO method.

This work was sponsored by the Polish National Committee for Scientific Research under the Wrocław University of Technology statutory funds.

References

Bürgi, H.-B. (1995). *Acta Cryst.* B**51**, 571–579.
Cole, J. M., Wilson, C. C., Howard, J. A. K. & Cruickshank, F. R. (2000). *Acta Cryst.* B**56**, 1085–1093.
Cruickshank, D. W. J. (1956). *Acta Cryst.* **9**, 754–756.
Dunitz, J. D., Maverick, E. F. & Trueblood, K. N. (1988). *Angew. Chem. Int. Ed. Engl.* **27**, 880–895.
Dunitz, J. D. & White, D. N. J. (1973). *Acta Cryst.* A**29**, 93–94.
Farrugia, L. (1997). *J. Appl. Cryst.* **30**, 565.
Farrugia, L. (1998). *WinGX-A*. University of Glasgow, Scotland.
Hołderna-Natkaniec, K., Khavryuchenko, V. D., Natkaniec, I., Szostak, M. M. & Wójcik, G. (1996). *Proceedings of the NATO Advanced Research Workshop 'ERPOS-7': Electrical and Related Properties of Organic Solids*, Polanica Zdrój, p. 94. Technical University, Wrocław, Poland.
Hummel, W., Raselli, A. & Bürgi, H.-B. (1990). *Acta Cryst.* B**46**, 683–692.
Jakubowski, B. & Ecolivet, C. (1980). *Mol. Cryst. Liq. Cryst.* **62**, 33–40.
Kuma Diffraction (1999). *Kuma KM4CCD Software.* Version 1.61. Kuma Diffraction, Wrocław, Poland.
Misiaszek, T., Girard, A. & Szostak, M. M. (1995). *Proceedings of the 10th International Conference on Fourier Transform Spectroscopy*, Budapest, Hungary. 1.28. Budapest: Hungarian Academy of Sciences.
Oudar, J. L. & Chemla, D. S. (1975). *Opt. Commun.* **13**, 164–168.
Perrin, M., Bavoux, C. & Thozet, A. (1977). *Acta Cryst.* B**33**, 3516–3519.
Perrin, M., Thozet, A., Lecoq, R., Perrin, R. & Lamartine, R. (1983). *Proc. SPIE*, **400**, 176.
Rohleder, J. W., Jakubowski, B. & Szostak, M. (1971). *Acta Phys. Pol.* A**40**, 777–783.
Schomaker, V. & Trueblood, K. N. (1968). *Acta Cryst.* B**24**, 63–76.
Schomaker, V. & Trueblood, K. N. (1998). *Acta Cryst.* B**54**, 507–514.
Sheldrick, G. M. (1990). *Acta Cryst.* A**46**, 467–473.
Sheldrick, G. M. (1997). *SHELXL*97. University of Göttingen, Germany.
Szostak, M. M., Misiaszek, T., Roszak, S., Rankin, J. G. & Czernuszewicz, R. S. (1995). *J. Phys. Chem.* **99**, 14992–15003.
Trueblood, K. N. (1978). *Acta Cryst.* A**34**, 950–954.
Turrell, G. (1972). *Infrared and Raman Spectra of Crystals.* London/New York: Academic Press.
Wójcik, G. & Holband, J. (2001). *Acta Cryst.* B**57**, 346–352.
Wójcik, G., Jakubowski, B., Szostak, M. M., Hołderna-Natkaniec, K., Mayer, J. & Natkaniec, I. (1992). *Phys. Status Solidi A*, **134**, 139–150.
Wójcik, G., Misiaszek, T. & Szostak, M. M. (1995). *Proceedings of the Polish Conference 'Molecular Crystals'*, Kiekrz, p. P-68. Institute of Molecular Physics, Polish Academy of Sciences, Poznan, Poland.
Wójcik, G., Szostak, M. M., Misiaszek, T., Pająk, Z., Wąsicki, J., Kołodziej, H. A. & Freundlich, P. (1999). *Chem. Phys.* **249**, 201–213.